ELSEVIER

Atmospheric Research 66 (2003) 65–82

ATMOSPHERIC RESEARCH

www.elsevier.com/locate/atmos

New satellite sensor and method for the direct measurement of the planetary albedo, results for 1999, 2000 and 2001 in South America

Nelson Veissid*

Laboratório Associado de Sensores e Materiais/CTE/INPE, C.P. 515, CEP 12201-970, São José dos Campos, São Paulo, Brazil

Received 27 November 2001; accepted 11 September 2002

Abstract

The second satellite of the Brazilian Complete Space Mission (SCD2/MECB) was launched on October 23, 1998 and it hosts a solar cell experiment. The solar cell senses visible radiation (400–1100 nm) and permits the simultaneous inference of direct insolation and the insolation that is reflected outside of the earth. The global albedo is obtained using the ratio between these two values after spherical angular corrections. The SCD2 has a circular orbit 750 km high and its spin is 35 rpm.

The solar cell data are transmitted in real-time and received by the ground station of Cuiabá, MT-Brazil (16°S, 56°W), which limits their spatial coverage to South America. The albedo data can be grouped in periods of time (annual, seasonal or monthly) or studied for several places during the orbit time. A new method to obtain the planetary albedo is tested through a numerical simulation using the data (cloud and land area) extracted from a GOES image. The solar cell experiment albedo values are shown as a function of SCD2 satellite orbit time to six local in South America. The values are in the range between 6% and 68%. The statistic analysis of the main values (minimum, maximum, mean and deviation) is done for 1999, 2000 and 2001. The results show several climate characteristics. For example, Recife-PE (8°S, 35°W) has good weather nearly all-year round. São Paulo (24°S, 47°W), in contrast, is famous for weather instability, with temperatures governed by cold fronts that come suddenly from the south.

The described method for evaluating the planetary albedo of the earth starts from a simple and relatively inexpensive experiment and does not rely upon sensor calibration because the measure is

* Fax: +55-12-3945-6717.

E-mail address: veissid@las.inpe.br (N. Veissid).

PII: S0169-8095(02)00157-6

self-calibrated by the simultaneous reading of both irradiation peaks, namely, from the sun and its reflection by the earth, during each spin of the satellite.

Keywords: Insolation; Planetary albedo; South America

1. Introduction

The incoming solar radiation that is reflected from the earth's surface and its atmosphere is generally called albedo. The albedo value depends on the nature, or quality, of the atmosphere and of the earth's surface, solar position and time. For instance, several phenomena (greenhouse effect, atmospheric temperature, inversion, aerosols, deforestation, volcanic eruption and others) alter the value of the albedo.

Aerial albedo measurements were apparently first made by Fritz (1948) with two pyrheliometers installed in a B-29 airplane. One was mounted on the top of the airplane to measure the downwelling solar radiation within the atmosphere. The other was mounted on the bottom to measure the upwelling component of solar radiation, which is the radiation reflected by the earth–atmosphere system. The albedo values along the flight path were determined by the quotient between these measurements after some corrections (Fritz, 1948). Fritz (1948) found that the ground (soil) albedo varied from 7% to 12%, and was occasionally higher than 29% when the ground was partially snow covered. Fritz (1950) also found that stratocumulus clouds had albedos higher than 80%.

Planetary albedo is the albedo measured outside of the earth–atmosphere system. Planetary albedo is the main parameter to calculate the solar energy radiation budget (ERB) in the earth. For example, Jacobowitz et al. (1979) reported on measurements of the Nimbus 6 satellite that has monitored the solar radiation input and the reflected shortwave and emitted longwave radiation exitance from the earth–atmosphere system. Jacobowitz et al. (1979) found a dip in the net radiation curve to earth in November, December and January and explained that it was due to the stronger outgoing radiation (reflected solar radiation plus emitted longwave radiation) that occurs at this period of the year. This was caused by an increase in the reflected radiation due in part to an increase in the albedo and in part to an increase in the incoming solar radiation. House et al. (1986) reported histories about several ERB satellite experiments until 1984 and concluded that measurements using nonscanning radiometers are better for measuring of the planetary albedo. The solar cell experiment of the SCD2 satellite is a nonscanning wide field of view (WFOV) sensor. At the moment, a new NASA satellite, called Terra, is monitoring the earth with passive sensors (King and Herring, 2000). The moderating-resolution imaging spectroradiometer (MODIS) is generating data for the production of a 1 km albedo standard data product. Evaluation of this product will allow an improved parameterization of radiometric exchanges at the earth's surface. Usually, the albedo is also obtained through data from digital cameras and scanning radiometers on geostationery satellites (GOES and METEOSAT). The evaluation of the albedo through these systems involves the integration of several channels with different spectral

windows, and they are reliable only when compared with other data (House et al., 1986). The calibration process is a very complex and is as expensive as the satellite digital cameras and needs to be done frequently.

Albedo measurements require establishment of the space geometry and the angular characteristics of solar radiation (incident and reflected). King and Curran (1980), in a simulation experiment of the effect of a nonuniform planetary albedo on the interpretation of the radiometer signal onboard a satellite, have adopted a very useful geometrical model. This model considers the field of view of the radiometer and the earth–atmosphere system like a perfect sphere of radius R with the satellite positioned at a height h above the surface of the sphere. Fig. 1 shows a satellite located at latitude ϕ and local hour angle λ. The reflected flux density is function of location on the globe, as shown below

$$F^{+}(\alpha,\zeta) = F_0 a(\alpha,\zeta)\cos\theta_0, \text{ to } \theta_0 < 90^\circ, \tag{1}$$

where F_0 is the solar flux density incident at the top of the atmosphere, a is the albedo of the earth–atmosphere system and θ_0 is the solar zenith angle at any particular location with coordinates α and ξ around the subsatellite point (see Fig. 1).

A satellite radiometer is only capable of estimating the mean flux density within the instantaneous field of view of the sensor. For the case of a nadir-looking radiometer with a

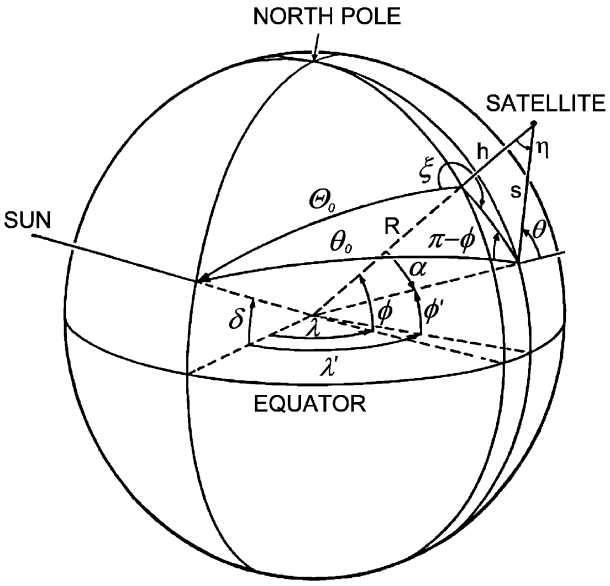

Fig. 1. Schematic illustration of the earth–atmosphere system illuminated by the sun at solar declination angle δ and viewed by a satellite at height h above the atmosphere. The angles and distances in this figure are discussed in the text (adapted from King and Curran, 1980).

circular field of view, the mean reflected flux density (F_{true}) within the field of view of the radiometer is given by

$$F_{\text{true}} = \frac{\int_0^{2\pi}\int_0^{\alpha_m} F^+(\alpha,\zeta)R^2\sin\alpha\,\mathrm{d}\alpha\mathrm{d}\zeta}{\int_0^{2\pi}\int_0^{\alpha_m} R^2\sin\alpha\,\mathrm{d}\alpha\mathrm{d}\zeta}$$

$$= \frac{1}{2\pi(1-\cos\alpha_m)}\int_0^{2\pi}\int_0^{\alpha_m} F^+(\alpha,\zeta)\sin\alpha\,\mathrm{d}\alpha\mathrm{d}\zeta, \tag{2}$$

where α_m is the instrument's instantaneous field of view. The measured flux density at satellite altitude differs from the true flux density at the top of the atmosphere. This is due to the nadir-looking sensor having an angular response function of cos η, where η is the angle at the satellite between the satellite nadir direction and the direction of an element of area on the surface of the sphere (see Fig. 1). The measured flux density is given by

$$F_{\text{meas}} = \frac{1}{\pi}\int_0^{2\pi}\int_0^{\alpha_m} F^+(\alpha,\zeta)\chi(\alpha,\varepsilon)\sin\alpha\,\mathrm{d}\alpha\mathrm{d}\zeta. \tag{3}$$

The factor $\chi(\alpha,\varepsilon)$ is azimuthally independent and acts to weigh the reflected intensity field incident on the satellite sensor (King and Curran, 1980) and ε is

$$\varepsilon = \frac{R+h}{R}. \tag{4}$$

King and Curran (1980) have considered the atmosphere within the field of view consisting of a large number N of equal area elements, and each area element has a plane albedo a_i. Fig. 2 illustrates the grid system used in the King and Curran (1980) investigation to calculate the simulated value of the albedo. Using this grid geometry, the measured flux density, Eq. (3), and the true flux density, Eq. (2), can be written as

$$F_{\text{meas}} = \frac{F_0}{\pi}\left(\cos\Theta_0\sum_i A_i a_i + \sin\Theta_0\sum_i B_i a_i\right) \tag{5}$$

$$F_{\text{true}} = \frac{F_0}{2\pi(1-\cos\alpha_m)}\left(\cos\Theta_0\sum_i C_i a_i + \sin\Theta_0\sum_i D_i a_i\right). \tag{6}$$

The elements (A_i, B_i, C_i and D_i) are analytically derived and can be found in the Appendix of the King and Curran (1980) work. The quantity F_{true} is ever higher than F_{meas} and this difference is due to angular response characteristics of the sensor, solid angle effects due to geometry and reflectance effects of the earth–atmosphere system. Jacobowitz et al. (1979) related these through a simple law involving only the satellite altitude given by

$$F_{\text{true}} = \varepsilon^2 F_{\text{meas}}. \tag{7}$$

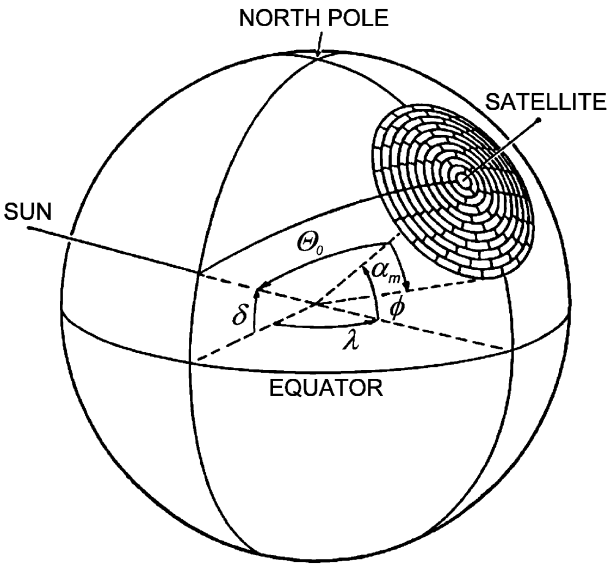

Fig. 2. Schematic illustration of the coordinate system used to simulate the reflectance within field of view of a satellite sensor (adapted from King and Curran, 1980).

King and Curran (1980) have calculated this relation as a function of the sensor field of view, solar zenith angle and, of course, satellite altitude. The equivalent expression for the SCD2 satellite, which has an altitude of 750 km and an $\varepsilon^2 = 1.24$, is

$$F_{\text{true}} = 1.19 F_{\text{meas}}. \tag{8}$$

Eq. (8) is used in this work to evaluate the true albedo. The King and Curran (1980) work also shows that only the solar cell experiment (SCE) data with solar zenith angle lower than 70° must be considered to calculate the albedo.

Photovoltaic sensors are very useful in the field of solar radiation measurement (Iqbal, 1983). The solar cell is a large area photovoltaic device, and solar cell of homojunction monocrystaline silicon has good spectral response between 400 and 1100 nm. The photo-generated current of this kind of sensor is proportional to the power of the solar radiation (Rauschenbach, 1980). Solar cell experiments have been used on some satellites (Huang et al., 1985; Veissid et al., 1997) to do space qualification of fabrication processes and devices. These kinds of experiments can be separated into two classes. The first corresponds to those with three axes orientation, where the solar panels are guided always to the sun. Unfortunately, this class is not usable as an albedo meter because the sun and the earth are not simultaneously viewed. The second class is related with satellites that have spin attitude control. Since spin attitude control allows for simultaneous viewing of the sun and earth, this second class of experiments is very useful for determining accurate albedo values. This fact avoids problems with temperature sensor and calibration in the measurement of albedo. The solar cell experiment (SCE) in the satellite SCD2 of INPE has a signal

conditioning circuit that reads the tension in the terminals of the cell and transmits this value by telemetry. Therefore, it is possible to measure the albedo as will be shown below.

2. Solar cell experiment description

The SCD2 is a collect and transmitter meteorological data satellite. The data are received from the terrestrial platforms distributed along the Brazilian territory and they work in a remote way, because some of them are located in places of difficult access. The orbit of SCD2 is 750 km in height and inclined around 25° in relation to the plane of the equator. The spin satellite is around 34 rpm. Its spin axis is maintained normal to the plane of celestial equator. The satellite is only illuminated by the sun during 65 min of each 100-min-long orbit. It is otherwise eclipsed by the shadow of the earth.

The solar cell experiment (SCE) is located at the lateral panel of the satellite and has a view angle of 180° (Fig. 3) because it has no collimation optical system. The SCE is composed of an arrangement of six connected solar cells of two by two in series. The solar cell is a semiconductor structure n+/p/p+ type manufactured in silicon substract with resistivity of 1 Ω cm. The description of this device can be found in Veissid and Pereira (2000). The array of solar cells is put on the aluminum mechanical structure.

The printed circuit board has the electronic components for conditioning signal. The array is composed of three pairs of cells and used to operate in three different conditions. The first one simulates the condition of short circuit current. That is, the terminals of the solar cell are connected to a load resistance of 1 Ω and this resistance supplies a tension that is amplified for a maximum value of 5 V. The value of this tension has the same magnitude of the short circuit current. The second pair has a load resistance of 8 Ω and it is

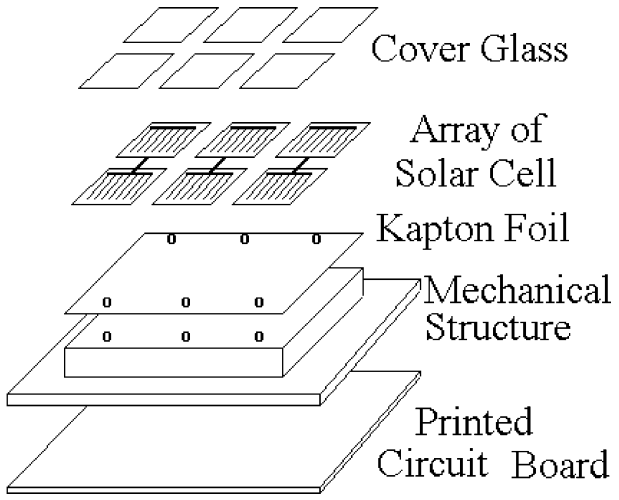

Fig. 3. Structural diagram of the SCD2/INPE solar cell experiment (SCE).

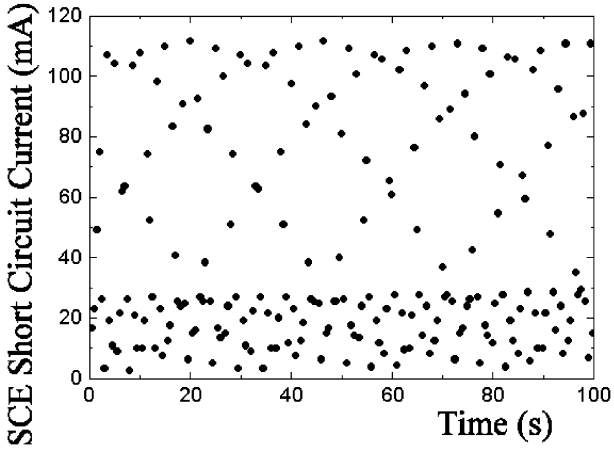

Fig. 4. Sample of SCE data received by satellite telemetry on November 21, 1998 at the 16:02 h GMT. The points are shown at half-second intervals.

linked to a second amplifier, to simulate the situation of maximum power. The third is the open circuit condition. This work only considers the short circuit current of the solar cell's array pair, because this current value is proportional to the light intensity, whether it is directly from the sun or reflected by the earth. The SCE telemetry module reads the value of the solar cells tension/current at each half-second, and due to the spin of the satellite, the values are distributed such as in Fig. 4.

Data of SCE are received at real-time only when the satellite is in the ground station field of view located at Cuiabá (16°S, 56°W), MT-Brazil. Unfortunately, this limits the

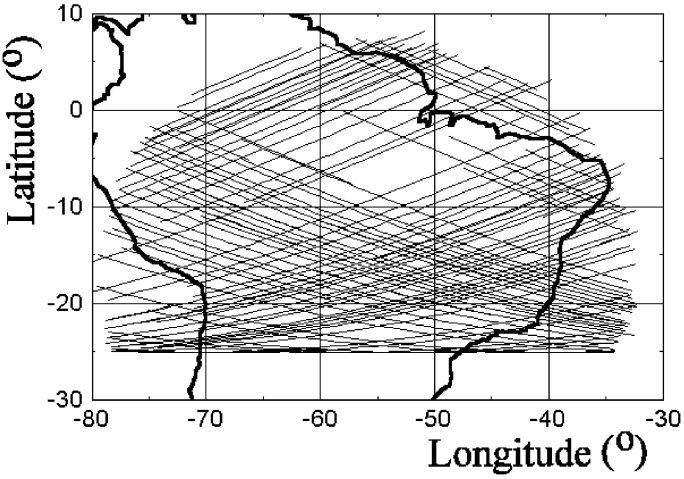

Fig. 5. SCD2 satellite orbits during November 1998 within the visibility range of Cuiabá ground station (16°S, 56°W).

SCE's observation range to the South American continent (i.e., latitude between 10°N and 30°S and longitude between 30°W and 80°W). Fig. 5 shows some SCD2 satellite orbits seen by ground station during November 1998.

3. Methodology

The values of short circuit current are plotted as a function of the orbit time (Fig. 4). Considering the exact value of the satellite spin during the measurement of these points and transforming the variables from time to satellite spin phase angle, we obtain the curve that is given by Fig. 6. The curve in Fig. 6 shows a dichotomy between the direct solar radiation and the reflected solar radiation by the earth. The satellite has its spin axe normal to the celestial equator plane, which is the plane of the earth's orbit around the sun, and this geometry yields two solar radiation peaks in the SCE curve: directly from the sun (higher, A_s) and reflected from the earth (lower, A_r). The algorithm used to calculate the albedo is the quotient between the magnitudes of the both peaks, with geometric corrections.

The solar flux density incident on the solar cell experiment is a function of the solar peak (A_s) and is mathematically expressed as

$$F_{SCE} = CA_s, \tag{9}$$

where C is a proportionality constant dependent of temperature and sensor area. This constant is a characteristic parameter of each solar cell and converts the units of the solar energy (mW/cm^2) into the units of short circuit current (mA) (e.g. Rauschenbach, 1980).

The solar flux density (F_0) is obtained considering the effective SCE's area illuminated by the solar rays and it is calculated using the attitude angle (α_{sat}) of the platform hosting the SCE (see Eq. (10)). The α_{sat} is the angle between spin axis of the satellite and the direction of solar rays. Its value is supplied by the CCR/INPE (Track and Satellite Control

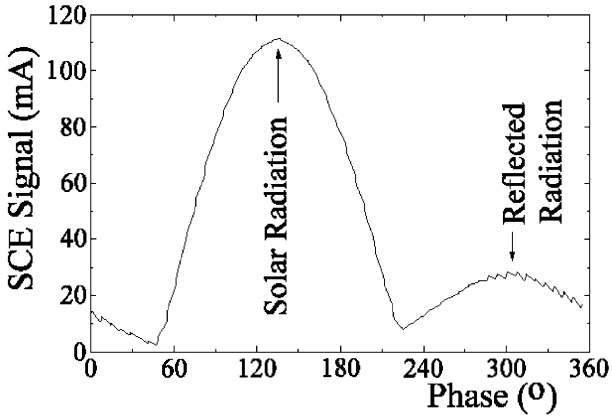

Fig. 6. Data of SCE of Fig. 5 after the variable changed from time to satellite spin phase.

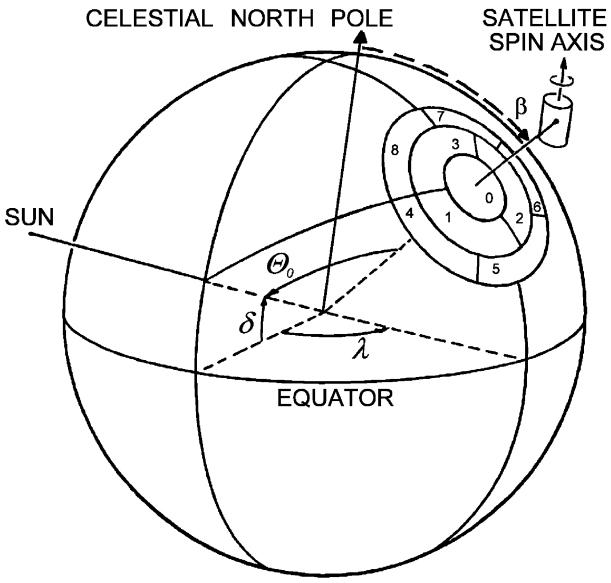

Fig. 7. Schematic illustration of the coordinate system used to simulate the reflectance of the SCD2/INPE satellite solar cell experiment (adapted from King and Curran, 1980).

of the INPE) of the SCD2 satellite together with the SCE data. Normally, the α_{sat} value is around $90 \pm 10°$.

$$F_0 = \frac{F_{SCE}}{\sin\alpha_{sat}} \tag{10}$$

The reflected solar flux density (F^+) is a function of the reflected solar peak (A_r) and the orientation of the satellite spin axe, which is ever appointed to the celestial north pole, with the nadir at the subsatellite point (β) (see Fig. 7). The β angle is calculated considering the longitude and latitude at the subsatellite point, the local hour and the solar declination is described by Iqbal (1983). The F^+ is given by

$$F^+ = \frac{CA_r}{\sin\beta} \tag{11}$$

The measured albedo is obtained using Eqs. (1), (9), (10) and (11), and is given by

$$a_{meas} = \frac{F^+}{F_0\cos\Theta_0} = \frac{A_r\sin\alpha_{sat}}{A_s\sin\beta\cos\Theta_0}. \tag{12}$$

The true albedo is obtained using the relation between F_{true} and F_{meas} (Eq. (8)) and is given by

$$a_{true} = 1.19a_{meas} \tag{13}$$

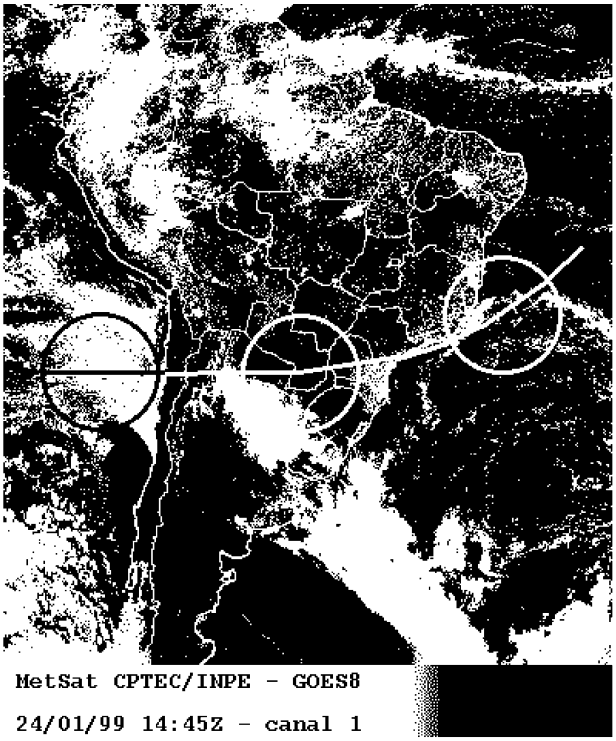

Fig. 8. Image of GOES-8 satellite obtained in the visible (VIS) spectrum, channel 1. The orbit track of the SCD2 satellite is the solid line.

In this way, the absolute albedo obtained by the solar cell experiment spectral range (400–1100 nm) is given by Eq. (13). From the data in Fig. 6, we have a value of $A_r/A_s = 0.24$ and an absolute/true albedo of 33%, calculated using Eq. (13), and obtained

Table 1
Data extracted from Fig. 8 and the estimated albedo calculated using Eq. (14)

Latitude (°S)	Longitude (°W)	Cloud fraction (%)	Land fraction (%)	Ocean fraction (%)	Estimated albedo (%)
24.6	77.5	60	0	40	38
25.0	72.5	50	40	10	36
25.1	67.5	30	65	5	28
25.1	62.5	35	65	0	31
24.8	57.5	20	80	0	24
24.4	52.5	15	70	15	20
23.8	47.5	15	50	35	18
23.0	42.5	15	35	50	17
22.0	37.5	15	15	70	15
20.7	32.5	10	0	90	11

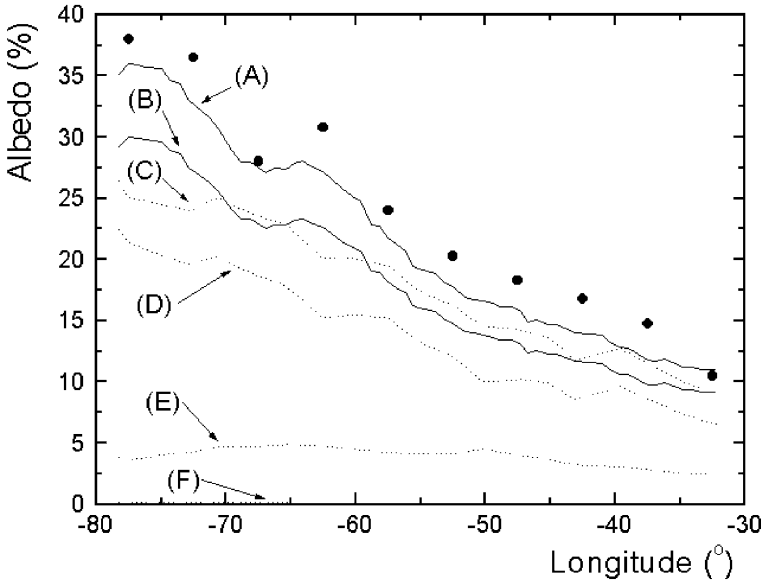

Fig. 9. Planetary albedo measured by SCE and the simulated curve using data from Fig. 8. The points (●) are the results of Table 1. Curve (A) is curve (B) multiplied by 1.19 (see Eq. (13)). Curve (B) is the albedo measured by the SCE according to Eq. (12). The curves (D), (E), and (F) correspond to the simulated albedo of the central circle, internal ring, and external ring, respectively (see Fig. 7). Curve (C) is the total simulated albedo, (D) plus (E) plus (F).

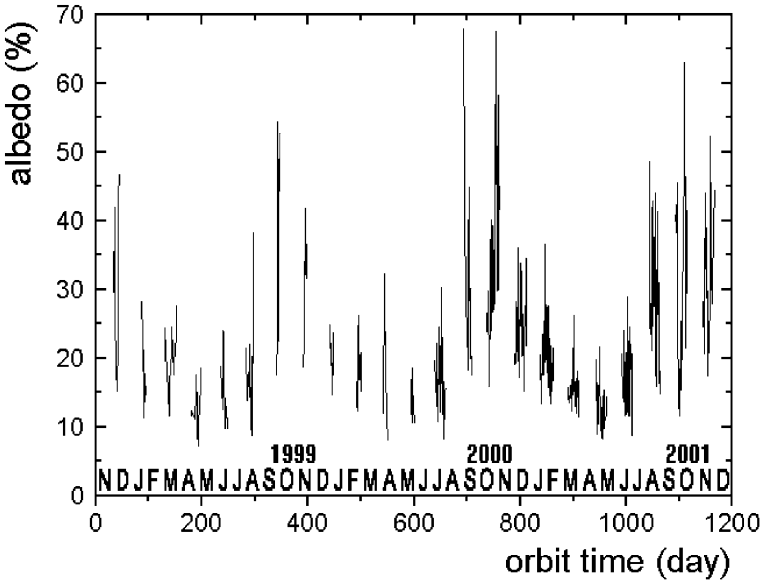

Fig. 10. Planetary albedo for São Paulo (24 ± 2°S, 47 ± 2°W) during 1999, 2000 and 2001.

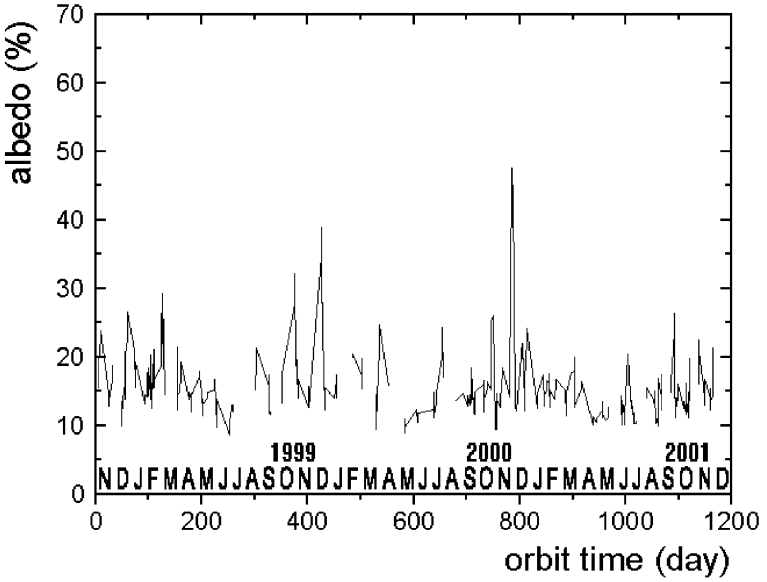

Fig. 11. Planetary albedo for Recife ($8 \pm 2°$S, $35 \pm 2°$W) during 1999, 2000 and 2001.

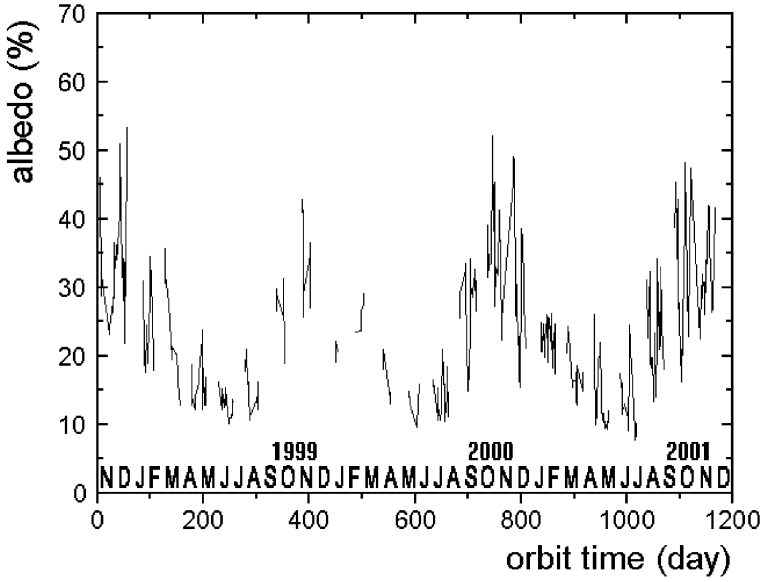

Fig. 12. Planetary albedo for Brasília ($16 \pm 2°$S, $48 \pm 2°$W) during 1999, 2000 and 2001.

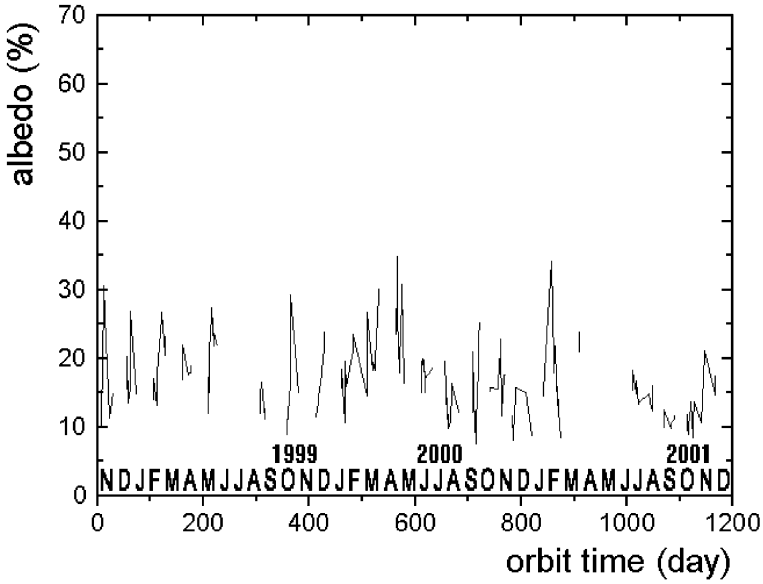

Fig. 13. Planetary albedo for the North Atlantic Ocean ($8 \pm 2°$N, $52 \pm 2°$W) during 1999, 2000 and 2001.

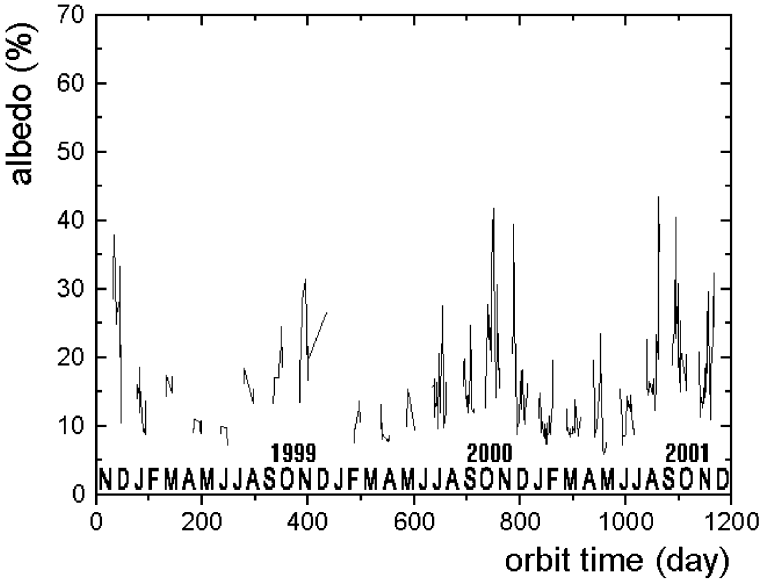

Fig. 14. Planetary albedo for the South Atlantic Ocean ($18 \pm 2°$S, $33 \pm 2°$W) during 1999, 2000 and 2001.

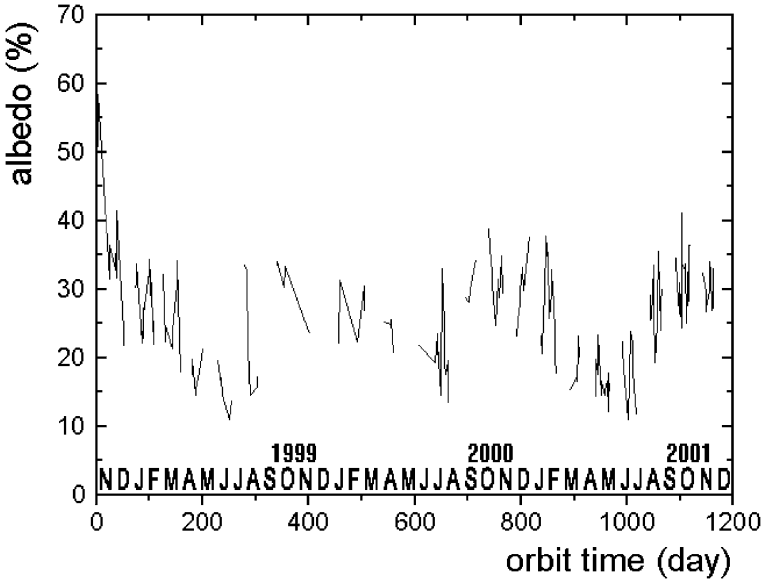

Fig. 15. Planetary albedo for the Titicaca Lake (16 ± 2°S, 69 ± 2°W) during 1999, 2000 and 2001.

from the 16:02 h GMT November 21, 1998 (3°52′S and 73°17′W) satellite data download.

4. Crude numerical albedo simulation

A simple numerical simulation was done using a GOES 8 channel 1 image of a partly cloudy area on January 24, 1999 at 14:45 GMT (Fig. 8). This section is called "crude numerical albedo simulation" since homogeneous albedo values for clouds, land and ocean were considered to be 60%, 15% and 5%, respectively. These do not correspond to reality. For example, the albedo for land is not similar to that for forest and soil. Fig. 8 shows the satellite orbit track, where 10 points are chosen in longitudes from 77.5° to 32.5°W with step of 5°. Fig. 8 has only three of these 12° diameter circles. Table 1

Table 2
Planetary albedo yearly values on São Paulo (24 ± 2°S, 47 ± 2°W) for 1999, 2000 and 2001, based on data from Fig. 10

Planetary albedo (%)	1999	2000	2001
Minimum	7.2	8.1	8.2
Maximum	54	68	63
Mean	21	26	23
Deviation	10.5	12.8	10.1

Table 3
Planetary albedo yearly values on Recife (8 ± 2°S, 35 ± 2°W) for 1999, 2000 and 2001, based on data from Fig. 11

Planetary albedo (%)	1999	2000	2001
Minimum	8.5	8.9	9.9
Maximum	39	48	26
Mean	16.5	16.5	14.8
Deviation	5.4	7.4	3.5

shows the surface proportion inside of each circle, which is estimated from Fig. 8, and the estimated albedo inside of each 12° diameter circle is calculated using the equation below.

$$a_{\text{esti}} = \frac{a_{\text{cloud}}S_{\text{cloud}} + a_{\text{land}}S_{\text{land}} + a_{\text{ocean}}S_{\text{ocean}}}{S_{\text{circle}}} \tag{14}$$

The parameters a and S are albedo and area, respectively. Table 1 also shows the value of estimated albedo calculated using Eq. (14).

The King and Curran (1980) geometrical model was adopted to simulate the albedo values found in the SCE experiment of the SCD2 satellite. The model uses a grid system such that each area element has exactly the same area. Fig. 7 illustrates the grid system used in the present work to assess the magnitude of the albedo within the field of view of SCE. It corresponds to a central circle with 18° diameter (named as segment number 0 in Fig. 7), an internal ring with 36° external diameter (composed by the segments numbers 1, 2 and 3) and an external ring with 52° (segments 4, 5, 6, 7 and 8). The estimated albedo of each segment is calculated using Eq. (14) and the data of Fig. 8. The simulated measured albedo values corresponding to the central circle, internal ring, external ring and total are plotted in Fig. 9, which are calculated using Eq. (5). Fig. 9 also shows the points of 12° diameter circle estimated albedo of Table 1. The simulated true albedo values are calculated using Eq. (8). Fig. 9 also shows both the experimental values of albedo, measured and true, by the SCE during the orbit track showed in Fig. 8. The curves of Fig. 9 show that the values have good correlation in spite of this crude numerical simulation. It is also possible to see that the method has a good potential to get better through a fitting technique in the SCE albedo curve.

It is interesting to emphasize that the true albedo seen by SCE, curve (A) in Fig. 9, is very close with the points of a 12° diameter circle estimated albedo (Table 1). This

Table 4
Planetary albedo yearly values on Brasília (16 ± 2°S, 48 ± 2°W) for 1999, 2000 and 2001, based on data from Fig. 12

Planetary albedo (%)	1999	2000	2001
Minimum	10.1	9.6	7.7
Maximum	43	52	48
Mean	20	24	23
Deviation	8.1	10.2	9.2

Table 5
Planetary albedo yearly values on the North Atlantic Ocean (8 ± 2°N, 52 ± 2°W) for 1999, 2000 and 2001, based on data from Fig. 13

Planetary albedo (%)	1999	2000	2001
Minimum	8.9	7.6	8.4
Maximum	29	35	34
Mean	17.8	17.9	14.3
Deviation	5.0	5.7	5.0

suggests that the SCE sees the reflected flux density below its satellite nadir direction with a strong response in the SCE signal.

5. The 1999, 2000 and 2001 results

The SCD2 satellite was launched on November 1998 and has provided several daily SCE data files. The SCD2, which is 750 km above the earth, takes 100 min to orbit the planet. We calculated the true albedo only when the solar zenith angle at the subsatellite point is lower than 70° and, normally, this corresponds in the local hour between 9:00 and 15:00 h. This provided 6 h of usable data for calculating albedo. All data were analyzed and they resulted in the temporal record of the albedo as a function of position. These data can be analyzed as a function of time (monthly, seasonal and annual) during the years of 1999, 2000 and 2001 for São Paulo, Recife and Brasília cities (Figs. 10–12, respectively) and for the North Atlantic Ocean, South Atlantic Ocean and on the Titicaca Lake (Figs. 13–15, respectively). The data were obtained within a geolocated area of ± 2° width in latitude and longitude. Tables 2–7 summarize the albedo variations during 1999, 2000 and 2001 for these locations.

The minimum value of albedo at Recife should be lower than that at São Paulo because of the larger ocean area at the field of view of SCE at Recife. However, the opposite result is found (e.g. Tables 2 and 3). São Paulo has problems with thermal inversion and, maybe, this provoked the low value of the albedo in May and June, which have lower albedo values. Another interesting conclusion is related with the standard deviation, which shows the weather variability. São Paulo city and region typically experience highly variable climate suggesting weather nonstability provoked by human influence. This information appears in a quantitative way in Table 2 and for comparing Fig. 10 with the other figures. The minimum albedo found in São Paulo was

Table 6
Planetary albedo yearly values on the South Atlantic Ocean (18 ± 2°S, 33 ± 2°W) for 1999, 2000 and 2001, based on data from Fig. 14

Planetary albedo (%)	1999	2000	2001
Minimum	7.3	7.6	5.8
Maximum	31	42	44
Mean	14.9	17.3	15.2
Deviation	5.9	7.9	6.8

Table 7
Planetary albedo yearly values on the Titicaca Lake (16 ± 2°S, 69 ± 2°W) for 1999, 2000 and 2001, based on data from Fig. 15

Planetary albedo (%)	1999	2000	2001
Minimum	11.0	13.2	10.9
Maximum	34	39	41
Mean	24	26	25
Deviation	6.7	5.9	7.3

on May 1999, the third day (autumn), and the inversion was probably very strong on this day.

Several climatic implications can be easily discussed by analyzing these SCE albedo data. For example, the variability (standard deviation) of the albedo in the cities of São Paulo and Brasília were higher. Why? We suppose that it represents an effect of global change or, maybe, it was only a temporary characteristic. Future data will be able to clarify this observation.

6. Conclusion

The SCE has no collimated optical system. It senses the luminosity in an instantaneous angle of view, which is theoretically at 180°. However, in a realistic way, this wide field of view is limited by the geometric condition of the SCD2 orbit. The entire earth–atmosphere system, horizon to horizon, is visible in the maximum central angle given by 26° (see Fig. 2). Eq. (3) has a factor that acts to weigh the SCE signal. This factor diminishes the wide field of view approximately to 4°. This consideration is based on the curve in the King and Curran (1980) work, which is almost a Gaussian curve, and the width at half-height is around 4°. So, we can say that the space resolution of the measured albedo seen by solar cell experiment is 5° or around 500 km in the equator. Nonetheless, it is a good sensor to infer planetary albedo because the data presents a general panorama of the albedo. It shows the planetary albedo with few details concerning a good space resolution, which is sometimes undesirable, mainly, for example, when the global change is being studied.

The albedo sensor described in this work is a by-product of an experiment with solar cells, whose main objective was to study radiation damage in this device. It is very interesting to observe that the sensor (solar cell or photodiode) is largely used as a radiation meter and the merit of the method is in the algorithm used for interpreting the data. Additionally, the method is self-calibrated by the numerical operation shown in Eq. (12).

According to Paul and Shukla (1994), the effects of deforestation can be separated into two categories: changes due to the change in vegetation alone, and changes due to albedo increase. The SCE data in the coming years will be able to identify the variation of albedo caused by deforestation in the Amazon rainforest.

Studies are being performed to develop this new methodology by including sensors with different spectral ranges in a future satellite experiment.

Acknowledgements

The author would like to acknowledge the Technological and Scientific National Council-CNPq, Brazilian governmental entity that promotes scientific and technological development, referent for the process number 46.7716/00-5. I am also grateful to Dr. A.F. Beloto for manufacturing of solar cells and to Dr. N.F. Leite for managing the sub-system during the year of 1993. The author acknowledges the OriginLab (http://www.originlab.com) for license to use his software in the data analysis of this work. Furthermore, the author would like to thank an anonymous referee whose careful reviews and comments regarding the model adopted led us to obtain better results.

References

Fritz, S., 1948. The albedo of the ground and atmosphere. Bulletin of the American Meteorological Society 29, 303.

Fritz, S., 1950. Measurements of the albedo of clouds. Bulletin of the American Meteorological Society 31 (1), 25.

House, F.B., Gruber, A., Hunt, G.E., Mecherikunnel, A.T., 1986. History of satellite missions and measurements of the Earth radiation budget (1957–1984). Review of Geophysics 24 (2), 357.

Huang, C., Wang, Q., Jiang, Q., 1985. Solar cell calibration experiment on Chinese scientific satellite. Proc. of the Eighteenth IEEE Phot. Spec. Conf., Las Vegas, USA, 634.

Iqbal, M., 1983. An Introduction to Solar Radiation. Academic Press, Canada.

Jacobowitz, H., Smith, W.L., Howell, H.B., Nagle, F.W., Hickey, J.R., 1979. The first 18 months of planetary radiation budget measurements from the Nimbus 6 ERB experiment. Journal of the Atmospheric Sciences 36, 501.

King, M.D., Curran, R.J., 1980. The effect of a nonuniform planetary albedo on the interpretation of Earth radiation budget observations. Journal of the Atmospheric Sciences 37, 1262.

King, M.D., Herring, D.D., 2000. Monitoring Earth's vital signs. Scientific American, 72 (April).

Paul, A.D., Shukla, J., 1994. Albedo as a modulator of climate response to tropical deforestation. Journal of Geophysical Research 99 (D10), 20863.

Rauschenbach, H.S., 1980. Solar Cell Array Design Handbook. Van Nostrand-Reinhold, New York.

Veissid, N., Pereira, E.B., 2000. A simple model for the assessment of the planetary albedo by using data from the solar cell experiment of the Brazilian SCD2 satellite. Brazilian Journal of Geophysics, 25.

Veissid, N., Nubile, P., Beloto, A.F., 1997. Results of the solar cell experiment of the first Brazilian satellite. Solar Energy Materials and Solar Cells 46 (1), 1.